Articles

Tyrosine 387 and Arginine 404 Are Critical in the Hydrolytic Mechanism of *Escherichia coli* Aminopeptidase P†

Shu-Chuan Jao, Li-Fang Huang, Shu-Mei Hwang, and Wen-Shan Li*

Institute of Chemistry, Academia Sinica, Taipei 115, Taiwan

Received September 5, 2005; Revised Manuscript Received December 9, 2005

ABSTRACT: Analysis of the pH−rate profile for catalysis of bradykinin cleavage by aminopeptidase P (AMPP), a manganese-containing hydrolase from *Escherichia coli*, was carried out to show that optimal catalytic function is obtained at neutral pH. On the basis of information derived from the crystal structure, peptidase sequence alignments, and the hydrolysis of organophosphate triesters, active site residues Arg153, Arg370, Trp88, Tyr387, and Arg404 were identified as potential catalytic residues. Site-directed mutagenesis was used to substitute these residues with Leu, Ala, Trp, Lys, or Phe. The k_{cat} values for the Arg153, Arg370, and Trp88 mutants were nearly the same as that for the wild-type enzyme. The k_{cat} values of the R404K, R404A, and Y387A mutants were lower by factors of 285, 400, and 16, respectively. Inductively coupled plasma mass spectrometry and circular dichroism spectroscopy showed that Arg404 is not required for metal chelation or stabilization of protein secondary structure. The hydrogen bond network observed between the side chains of conserved residues Asp260, Arg404, and Tyr387 indicated that Arg404 participates in proton relay. This was further evidenced by the return of activity in the R404A mutant by the addition of guanidine. Also, reduced catalytic efficiency in the R404K mutant, which conserves the positive charge at the bridge site, shows that only the arginine group of Arg404 (not the ammonium group of Lys404) can participate in the hydrogen bond network. The hydrogen bond interaction between the Arg404 and the Tyr387 ring hydroxyl group is suggested by the reduced catalytic efficiency of the Y387F mutant.

Escherichia coli aminopeptidase P (AMPP,[1] EC 3.4.11.9), a member of proline-specific peptidases, catalyzes the hydrolysis of the Xaa−Pro bond at the N-terminus of polypeptides (*1*−*7*). The X-ray structure of AMPP (*8*−*10*) shows that the enzyme is a tetramer with each subunit composed of the "pita-bread" fold of the C-terminal domain and an N-terminal domain of unknown function. Methionine aminopeptidase (EC 3.4.11.18) (*11*−*14*), creatinase (EC 3.5.3.3) (*15*−*17*), and prolidase (EC 3.4.13.9) (*18*−*20*) are also known to exhibit the pita-bread fold (*4*, *21*). Within this fold family, the aminopeptidases and prolidases, which cleave the Arg−Pro bond of bradykinin (Arg-Pro-Pro-Gly-Phe-Ser-Pro-Phe-Arg), are known to play important roles in pulmonary and coronary circulation (*22*, *23*). It has been shown that *E. coli* AMPP hydrolyzes bradykinin at a significantly faster rate than the dipeptides (Xaa-Pro). For example, the k_{cat}/K_m value for the hydrolysis of bradykinin is 46−643-fold higher than those for the hydrolysis of Arg−Pro and Tyr−Pro bonds (*1*). In addition, the enzyme preferentially cleaves tripeptides or longer polypeptides at very similar rates. The k_{cat} values for the hydrolysis of Arg-Pro-Pro, hermorphin (Tyr-Pro-Trp-Thr-Gln), β-casomorphin (Tyr-Pro-Phe-Pro-Gly-Pro-Ile), and bradykinin by *E. coli* AMPP were 76, 33, 64, and 69 s^{-1}, respectively (*1*).

Recent structural studies and electron paramagnetic resonance investigations of AMPP have shown that the Mn_A^{2+}−Mn_B^{2+} binuclear manganese cluster, located in the C-terminal domain, is critical for maximal catalytic activity of the enzyme (*2*−*8*). The two metal ions are separated by 3.3 Å. Mn_A^{2+} is positioned at the mouth of the active site through coordination to the side chains of Asp271, Glu383, His354, and Glu406. Mn_B^{2+}, which is coordinated to Asp260, Asp271, and Glu406, is buried in the active site cleft (Figure 1). The Mn^{2+} cofactor can be replaced by Co^{2+} with retention of enzyme activity but not by Mg^{2+}, Zn^{2+}, or Ca^{2+} (*7*). Recent studies have shown that the removal of the N-terminal domain from *E. coli* AMPP results in protein aggregation and activity loss and that, in addition to proteolysis, this enzyme catalyzes hydrolytic P−O bond cleavage in a variety of organophosphate triesters, including the insecticide paraoxon (*24*).

† This work was supported in part by the National Science Council (NSC 93-2113-M-001-035) and Academia Sinica (program project).

* To whom correspondence should be addressed. Phone: 886-2-27898662. Fax: 886-2-27831237. E-mail: wenshan@chem.sinica.edu.tw.

[1] Abbreviations: AMPP, aminopeptidase P; Tris, tris(hydroxymethyl)aminomethane; DTT, dithiothreitol; CD, circular dichroism; ICP-MS, inductively coupled plasma mass spectrometry; SDS−PAGE, sodium dodecyl sulfate−polyacrylamide gel electrophoresis; IPTG, isopropyl D-thiogalactopyranoside; HPLC, high-performance liquid chromatography; PCR, polymerase chain reaction.

10.1021/bi051786m CCC: $33.50
Published on Web 01/20/2006

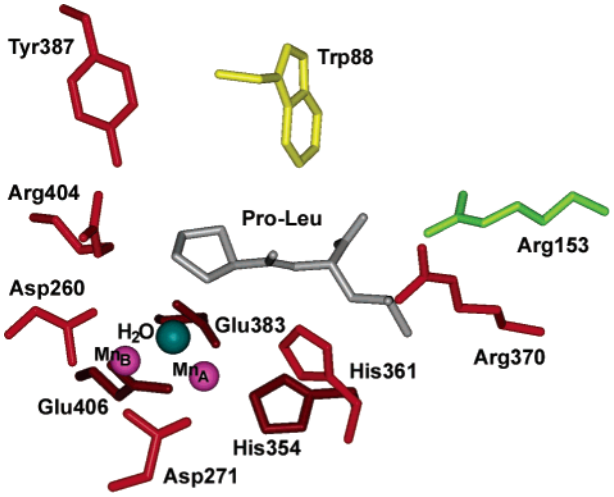

FIGURE 1: Binuclear manganese cluster of native AMPP with the Pro-Leu inhibitor bound. The inhibitor is colored gray. Four residues, Arg370, Arg153, Trp88, and Arg404, selected for point mutations from a different monomer (colored red, green, yellow, and red, respectively) are near the rim of the active site pocket. The coordinates are taken from the structure reported by Wilce (*8*).

	Residue Number		
	256-265	380-388	398-409
AMPP_Ec	LVLI**D**AGCEY	LTVEPGL**Y**I	RGI-GI**R**IEDDI
AMPP_Sl	LLLL**D**AGVET	LTVEPGL**Y**F	RGI-GV**R**IEDDI
AMPP_Mt	FVKI**D**FGALV	VTVEPGV**Y**L	PGRGGV**R**IEDTL
PepD_Hu	MCLF**D**MGGEY	LTVEPGI**Y**F	RGFGGV**R**IEEDV
PepD_Ec	SFLL**D**AGAEY	LTIEPGI**Y**F	KPFGGI**R**IEDNV

FIGURE 2: Sequences of various AMPPs and prolidases (PepDs), adapted from ref *4*. The residue numbering refers to that of AMPP_*Ec*. Conserved residues of interest, Asp260, Tyr387, and Arg404, described in the text are in bold characters. AMPP_Ec is aminopeptidase P from *E. coli* (Ec), AMPP_Sl aminopeptidase P from *Streptomyces lividans* (Sl), AMPP_Mt aminopeptidase P from *Mycobacterium tuberculosis* (Mt), PepD_Hu prolidase from human (Hu), and PepD_Ec prolidase from *E. coli* (Ec).

In this work, we examine the mechanism of *E. coli* AMPP catalysis and substrate binding. In an earlier publication (*8*), it was suggested that (1) Glu383 abstracts the proton from the bridging water to initiate nucleophilic attack at the carbonyl carbon of the peptide bond, (2) His361 polarizes the carbonyl group (C═O) of the Xaa−Pro bond to increase the electrophilicity of the carbon center, and (3) the leaving peptide is neutralized by abstracting a proton from the solvent. The mechanism of the proton transfer from solvent to the leaving group is addressed in this paper. The AMPP crystal structure shows that the positively charged guanidinium side chain of Arg404 is properly positioned to engage in hydrogen bond formation with the carboxylate side chain of Asp260 and with the ring hydroxyl group of Tyr387. A Mn_B Asp260···Arg404···Tyr387 hydrogen-bonded network might serve as the conduit for proton relay between solvent and the reaction center. Indeed, sequence alignments of three AMPPs and two prolidases show that these residues are conserved (Figure 2). To test the contributions made by Arg404 and Tyr387 to catalysis, site-directed mutants were constructed and their steady-state kinetic properties were evaluated.

The *E. coli* AMPP crystal structure also indicates that Arg153, Arg370, and Trp88 (each from a different monomer) are located in the vicinity of the bound inhibitor (Pro-Leu) and thus may play an important role in binding bradykinin, a potent cardioprotective peptide hormone. The roles of Arg153, Arg370, and Trp88 were evaluated by kinetic analysis of site-directed mutants. The results reported below provide evidence for the roles played by Arg404 and Tyr387 in the proton relay and rule out the participation of Arg153, Arg370, and Trp88 in substrate binding.

EXPERIMENTAL PROCEDURES

Materials. All buffers and chemicals were purchased from Sigma, Aldrich, or Acros Organics. The restriction endonucleases and DNA polymerase were purchased from New England Biolabs. The QuikChange Multi Site-Directed Mutagenesis Kit was from Stratagene. pET plasmids and *E. coli* strains were from Novagen. PD10 and HiTrap chelating columns were from Amersham Biosciences. Bradykinin was from Sigma and LB broth from Becton, Dickinson and Company. Primers were synthesized by MDBio Inc.

Site-Directed Mutagenesis of AMPP. pCJ03 was used as a template, and the QuikChange kit from Stratagene was utilized according to the manufacturer's instructions to give plasmids containing R153A, Y387F, R404A, and R404K mutants. The plasmids containing the desired mutations were confirmed by sequence analysis. Construction of the pCJ03 plasmid containing the DNA encoding *E. coli* AMPP, *pepP*, has been described previously (*24*). This plasmid is the pET15b expression vector with the *pepP* insertion flanked by *Nde*I and *Bam*HI restriction sites. The plasmid allowed production of AMPP as an N-terminal fusion with a hexahistidine tag in *E. coli* under control of the IPTG inducible T7 promoter. AMPP mutants R153L, R153W, and R370L were obtained as described previously (*24*). Double mutants R153L/R370L and R153W/R370L were prepared using the plasmid containing AMPP-R370L encoding DNA as the template. The only mutant not obtained from the QuikChange strategy was W88L because one of the desired primers contained secondary structure. Therefore, PCR-based site-directed mutagenesis was used. The plasmid containing the W88L mutant was confirmed by sequence analysis. To generate His-tagged free wild-type AMPP and the R404A mutant for inductively coupled plasma mass spectrometry (ICP-MS), the corresponding DNA of AMPP in the pET15b construct was subcloned into the pET22b vector utilizing *Nde*I and *Bam*HI restriction sites. Because the stop codon at the end of the *pepP* gene and the *Nde*I site of pET22b is located six bases downstream of the ribosome-binding site, the construct did not form His-tagged proteins.

Protein Expression and Purification. The expression and purification of His-tagged *E. coli* AMPP and its mutants have been described previously with minor modification. In brief, the plasmid containing the desired mutant was first transformed into *E. coli* BL21(DE3) competent cells. A single colony from the overnight plate was selected to inoculate a 50 mL culture, which was incubated to an OD_{600} of 1.0. An 18 mL aliquot was mixed with 2 mL of 80% glycerol and stored at −80 °C. The 20 mL frozen stock was used to inoculate 500 mL of LB medium containing the appropriate antibiotics for the plasmid at 37 °C. IPTG was added to a final concentration of 1 mM when the OD_{600} reached between 0.9 and 1.0. The cells were harvested after 3 h by centrifuga-

tion at 6000 rpm and stored at −80 °C. The cell pellet was suspended in 25 mL of 20 mM Tris-HCl (pH 7.4) and 0.2 mM DTT on ice and passed twice through a French press at 11 000 psi. Next, 5 M NaCl and 5 M imidazole were added to the cell lysate to adjust the concentration of NaCl and imidazole to 500 and 10 mM, respectively. The solution was centrifuged at 12 000 rpm for 20 min, and the supernatant was applied to a fully equilibrated 5 mL Ni^{2+} chelating column and purified according to the manufacturer's protocol. Fractions containing the desired protein were pooled and dialyzed overnight against 20 mM Tris-HCl (pH 8.2), 0.1 mM EDTA, and 0.1 mM DTT and then against two changes of the Tris buffer without EDTA and DTT. The resulting apoenzyme was stored in 20% glycerol at −80 °C. The wild type and R404A without a hexahistidine tag were expressed using the procedure described above for His-tagged AMPP, and the purification of the protein was carried out according to the method described in ref 7. The protein concentrations were determined spectrophotometrically in the 6 M guanidinium hydrochloride/20 mM potassium phosphate buffer (pH 6.5) by using the extinction coefficient at 280 nm calculated using ProtParam on the Expacy server (*25*).

Enzyme Assays. The rate of the reaction of the AMPP-catalyzing hydrolysis of bradykinin into the desired product, des-Arg-bradykinin (Pro-Pro-Gly-Phe-Ser-Pro-Phe-Arg), was assayed using a reverse-phase HPLC system (Waters 2695 Separations Module) equipped with an autosampler and UV−visible photodiode array detector, with monitoring at 215 nm. The reaction is shown in eq 1.

$$\text{bradykinin} + H_2O \rightarrow \text{des-bradykinin} + \text{L-arginine} \quad (1)$$

The enzyme was first activated with a 20-fold excess of $MnCl_2$ at 37 °C for 30 min and then added to the assay mixture containing bradykinin in 50 mM Tris-HCl buffer (pH 7.5) at 37 °C for 10 min. The reaction was terminated by heating the mixture for 5 min at 100 °C. Following centrifugation for 2 min, a 25 or 50 μL aliquot of the supernatant was analyzed by HPLC on a Vydac C18 column (5 μm, 25 cm × 4.6 mm) under a gradient running from 20 to 67% (v/v) acetonitrile containing 0.1% (v/v) trifluoroacetic acid over the course of 20 min. A control reaction without enzyme was analyzed in parallel. For kinetic analysis, assays contained a range of concentrations of bradykinin (100−3500 μM for W88L and 100−2500 μM for other mutants) and 2 nM wild-type or mutant (R153A, R153L, R153W, R370L, R153L/R370L, and R153W/R370L) enzyme. Mutants W88L, Y387F, R404A, and R404K, displaying lower peptidase activities, were added to the incubation mixture with higher concentrations: 25, 100, 1500, and 1500 nM, respectively. A representative chromatogram is depicted in Figure 3. The pH optimum for the hydrolysis reaction was determined over the pH range of 6.5−9.5 in 50 mM Tris-HCl buffer containing 2.5 mM bradykinin. To test the reactivation of the R404A mutant by guanidine, the apoenzyme of the R404A mutant (750 nM) was first incubated with a 50-fold excess of $MnCl_2$ at 37 °C for 30 min. The enzyme was then assayed for catalytic activity with 7.5 or 75 μM guanidine and 250 μM bradykinin in 50 mM Tris-HCl buffer (pH 7.5) at 37 °C for 10 min.

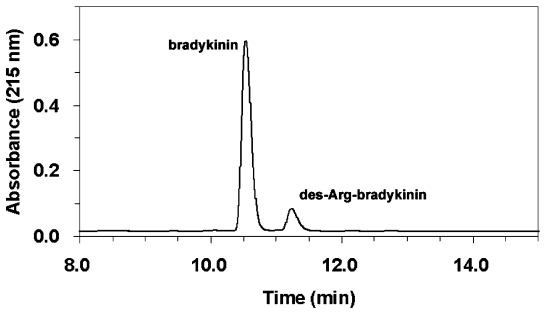

FIGURE 3: Representative RP-HPLC trace of bradykinin being hydrolyzed by wild-type AMPP (2 nM) monitored at 215 nm. The assay was performed at 37 °C in 50 mM Tris-HCl (pH 7.5) for 10 min, quenched by heating for 5 min at 100 °C, and subjected to HPLC.

The values of k_{cat}, K_m, and V_{max} were obtained by fitting the initial velocity data to eqs 2 and 3

$$v/E_t = k_{cat}S/(K_m + S) \quad (2)$$

$$v = V_mS/(K_m + S) \quad (3)$$

where v is the initial velocity, k_{cat} is the turnover number, K_m is the Michaelis constant, V_m is the maximum velocity, S is the substrate concentration, and E_t is the enzyme concentration.

Circular Dichroism (CD) of AMPP Mutants. CD spectra were obtained from 200 to 260 nm at 0.5 nm intervals using a Jasco J720 spectropolarimeter and a 0.2 cm cylindrical quartz cuvette. Protein samples were prepared at 0.1 mg/mL in 50 mM potassium phosphate buffer (pH 7.4). The spectrum for each sample was averaged over 10 acquisitions, and the background contributed by buffer was subtracted. The measured ellipticity data were converted into mean residue ellipticity, $[\theta]$, which is defined as $[\theta] = \theta/10nCl$, where θ is the measured ellipticity in millidegrees, l is the path length of the cuvette in centimeters, C is the molar concentration of enzyme subunits, and n is the number of residues per enzyme subunit (461 amino acids, including the His tag). The CD data were plotted as mean residue ellipticity $[\theta]$ (degrees square centimeters per decimole) against wavelength in 0.5 nm steps.

Inductively Coupled Plasma Mass Spectrometry (ICP-MS). The His tag-free enzyme (wild-type or R404A AMPP) was first activated by a 20-fold excess of Mn^{2+} at 37 °C for 30 min. The solution was then passed twice through a PD10 column equilibrated with 10 mM Tris buffer (pH 7.4). The PD10 fraction immediately preceding that containing protein was also analyzed for Mn^{2+} content as a buffer control. ICP-MS analysis was carried out at the Instrument Center of Hsinchu at National Tsing Hua University (Perkin-Elmer, SCIEX ELAN 5000). The protein concentrations used for ICP-MS analysis were 41.3 and 29.3 μM for wild-type and R404A AMPP, respectively.

RESULTS

Purity and Activity of AMPP Mutants. Ten mutants of AMPP were individually constructed by site-directed mutagenesis, employing a QuikChange strategy or a PCR-based method. The genes for these mutants were confirmed by DNA sequencing. The mutant proteins were expressed in *E.*

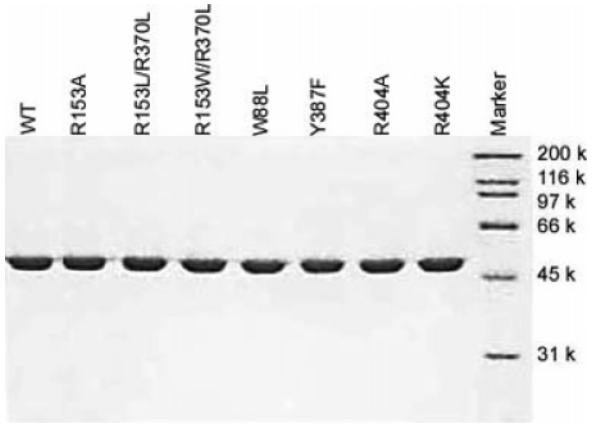

FIGURE 4: Coomassie R250-stained SDS−PAGE gel (10%) of Ni chelating column-purified mutant and wild-type AMPP (2.5 μg).

Table 1: Kinetic Parameters for Wild-Type and Mutant Enzymes[a]

enzyme	K_m (μM)	k_{cat} (s^{-1})	k_{cat}/K_m (M^{-1} s^{-1})
wild type	780 ± 60	69 ± 2	8.8×10^4
R153A	420 ± 50	72 ± 3	1.7×10^5
R153L	510 ± 50	109 ± 3	2.1×10^5
R153W	430 ± 60	70 ± 3	1.6×10^5
R370L	210 ± 20	102 ± 3	4.9×10^5
R153L/R370L	180 ± 10	57 ± 1	3.3×10^5
R153W/R370L	160 ± 20	87 ± 2	5.6×10^5
W88L	1020 ± 90	13.8 ± 0.4	1.4×10^4

[a] Assays were performed in the presence of bradykinin at 37 °C in 50 mM Tris-HCl buffer (pH 7.5) as described in Experimental Procedures (mean ± standard deviation).

coli strain BL(DE3) and purified by Ni^{2+} affinity chromatography to homogeneity as shown by the SDS−PAGE gel of Figure 4. Both wild-type AMPP and the R404A AMPP mutant lacking the hexahistidine tag were also purified. The extra amino acids at the N-terminus did not affect the hydrolysis activity of AMPP. Yields of overproduction ranged from approximately 40 to 60 mg/L. The R404L mutant was unstable and aggregated during purification, and attempts to refold it in the presence of Mn^{2+} and/or proline were not successful. In contrast, the R404A and R404K mutants were well-behaved.

Activity and Kinetic Characterization of AMPP Mutants. The X-ray crystal structure of AMPP indicates that Arg153, Arg370, and Trp88 are individually derived from different monomers. In previously published (*24*) and in recently published work on AMPP-catalyzed organophosphate ester hydrolysis, we have shown that the cavity lined with Trp88, Arg153, and Arg370 accommodates the *p*-nitrophenyl leaving group and orients the substrate to give the specificity. To understand the role of these residues in hydrolyzing the native substrate, the kinetic parameters of single and double mutants at residues Arg153, Arg370, and Trp88 in catalysis of bradykinin cleavage were measured. The results are reported in Table 1. Six of the mutants (R153A, R153L, R153W, R370L, R153L/R370L, and R153W/R370L) exhibited a 2−5-fold decrease in K_m and a 2−6-fold increase in k_{cat}/K_m relative to those of the wild-type enzyme. Wilce et al. found that Trp88 is one of the residues from a neighboring subunit that extends the rim of the active site pocket along with Phe89 and Asp38 (*8*). When this Trp88 is replaced with leucine, there is a 1.3-fold increase in the measured K_m. In addition, the k_{cat} and k_{cat}/K_m values of W88L AMPP were 5−6-fold lower than those of wild-type AMPP.

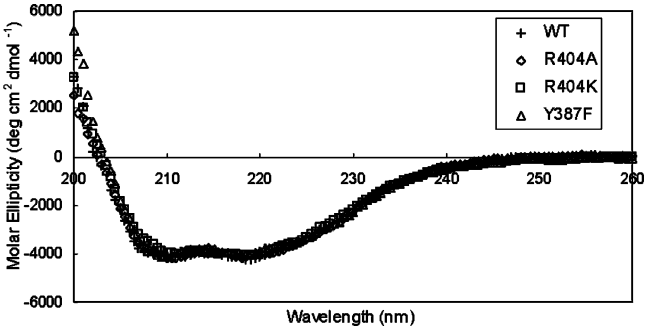

FIGURE 5: CD spectra of AMPP mutants.

Table 2: Steady-State Kinetic Parameters for AMPP and Arg404 and Tyr387 Variants

enzyme	K_m (μM)	k_{cat} (s^{-1})	k_{cat}/K_m (M^{-1} s^{-1})
wild type	780 ± 60	69 ± 2	8.8×10^4
R404A	47 ± 2	0.17 ± 0.00	3.7×10^3
R404K	410 ± 90	0.24 ± 0.01	5.9×10^2
Y387F	840 ± 80	4.2 ± 0.2	5.0×10^3

Arg404 and Tyr387 Are Required for Efficient Catalysis. Table 2 lists the k_{cat}, K_m, and k_{cat}/K_m values for R404A, R404K, and Y387F AMPP-catalyzed cleavage of bradykinin. The k_{cat} values of the Arg404 mutants were 285−400-fold lower than that of the wild-type enzyme. The K_m was decreased 17-fold in the R404A mutant and 2-fold in the R404K mutant. The Y387F AMPP K_m value was comparable to that of wild-type AMPP, whereas the k_{cat} value was decreased 16-fold.

Circular Dichroism (CD) Spectra of Purified AMPP Mutants. CD spectra (Figure 5) were obtained for wild-type AMPP and the catalytically impaired mutants R404A, R404K, and Y387F in the presence of Mn^{2+} to determine whether the secondary structure of the native enzyme was retained in the mutants. CD spectral analysis showed two minima at 208 and 220 nm, which are indicative of a predominance of α-helical structure. No major differences were detected in CD spectra measured from 200 to 260 nm, indicating that no substantial changes in the backbone fold had resulted from the single-amino acid substitutions made in the respective mutants.

Mn^{2+} Stoichiometry in Wild-Type and R404A AMPP. The three-dimensional X-ray structure of AMPP reveals paired Mn^{2+} ions (*8*). To test whether the low activity of R404A might be due to loss of Mn^{2+}, inductively coupled plasma resonance mass spectrometry (ICP-MS) was used to measure the metal content of the mutant and wild-type enzyme. Wild-type AMPP and R404A AMPP were expressed and purified without a hexahistidine tag. The ICP-MS data demonstrate that R404A AMPP and wild-type AMPP bind manganese with a stoichiometry of 2.03 ± 0.02 and 2.16 ± 0.06 per monomer, respectively. This result shows that the low activity of the R404A mutant is not due to the loss of Mn^{2+} ion.

Activation of the R404A Mutant by Guanidine. Wild-type, R404A, and R404K AMPP were assayed for peptidase activity in the presence of different concentrations of guanidine. The specific activity of the R404A mutant was increased from 0.17 to 0.35 μmol min^{-1} mg^{-1} in the presence of 7.5 μM guanidine and to 0.95 μmol min^{-1} mg^{-1} in the

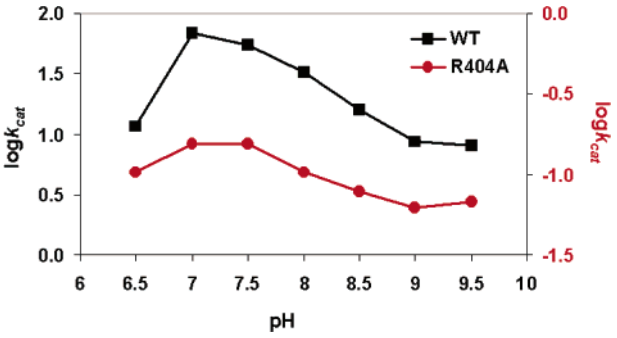

FIGURE 6: pH dependence of log k_{cat} for R404A (●) and wild-type (■) AMPP. Values of log k_{cat} were determined in the pH range of 6.5−9.5 as described in Experimental Procedures.

Chart 1

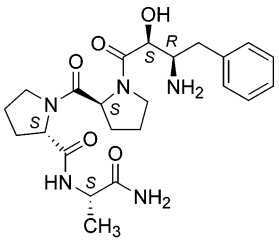

Apstatin

presence of 75 μM guanidine. In contrast, the activities of wild-type AMPP and R404K AMPP were not affected by the guanidine.

pH−Rate Profiles. To study the effect of pH on k_{cat}, wild-type AMPP and R404A AMPP were investigated in the pH range from 6.5 to 9.5. The wild-type enzyme exhibited a bell-shaped pH dependence with an optimal pH of ~7.0 (Figure 6). The R404A mutant, in which the arginine side chain was replaced with a methyl group, exhibited a pH−rate profile similar to that of the wild-type enzyme.

DISCUSSION

The studies of *E. coli* AMPP-catalyzed hydrolysis of bradykinin, described above, show that mutation of either Arg153 or Arg370 leads to a 2−5-fold decrease in the K_m value. However, there is no significant difference in the magnitude of k_{cat}. The X-ray structure of the Pro-Leu−AMPP complex (*8*) shows the guanidinium groups of Arg370 and Arg153 form hydrogen bonds or salt bridges with the carboxylate group of the Pro-Leu inhibitor. Substitution of these residues appears to weaken substrate binding and, thus, leads to increased K_m values. Obviously, the interactions between bradykinin and the side chains of Arg153 and Arg370 are different compared to those involved in binding to Pro-Leu. On the other hand, the X-ray structure of the apstatin {*N*-[(2*S*,3*R*)-3-amino-2-hydroxy-4-phenylbutanoyl]-L-prolyl-L-prolyl-L-alaninamide; see Chart 1}−AMPP complex (*10*) shows that Arg370 is located in the vicinity of the second Pro residue of apstatin, whose position might be similar to P_2' of bradykinin. In addition, this structure shows that Arg153 is close to a Pro and Ala residue. Mutation of arginine to alanine, leucine, and tryptophan could enhance hydrophobic interactions between the side chains in the mutants and the P_2', P_3', and P_4' (Pro, Gly, and Phe, respectively) positions of bradykinin. In general, the existence of positive charges on the two residues is not necessary for binding of bradykinin, but their interference does not affect the catalytic activity.

Trp88 and the catalytic Mn^{2+} ions are located on different subunits of this enzyme. The 5-fold lower k_{cat} and the 1.3-fold higher K_m for W88L indicate that this mutation alters hydrophobic interactions between the enzyme and bradykinin by replacing the Trp side chain with a smaller Leu residue. This substitution also might change the orientation of the Arg−Pro bond of bradykinin relative to the binuclear metal center. This might be the reason Trp88 substitution leads to a higher K_m value and a lower k_{cat}.

The mutants containing a substitution for Arg404 have a significantly lower rate of hydrolysis of bradykinin (285−400-fold decrease in k_{cat}), indicating that this residue is essential for catalytic activity. Although Leu substitution at this position results in protein aggregation, Ala or Lys substitution does not pose this problem. These observations suggest that the crowded active site environment cannot accommodate larger hydrophobic groups. Interestingly, the binding affinity of AMPP is enhanced by ca. 17-fold if Arg404 is replaced with alanine (Table 2). The observed decrease in K_m can possibly be explained by considering that the change from arginine to alanine creates a cavity that is able to accommodate the N-terminal Arg of bradykinin. However, while this replacement enhances binding affinity, it may simultaneously reorient the Arg−Pro bond of bradykinin away from important catalytic residues and, thus, cause a lower catalytic activity.

The guanidinium group of Arg404 presents a positive charge near the active site pocket and potentially strengthens the electrostatic repulsion between the arginine moiety of the substrate and the arginine in the active site. We constructed R404K, having a lysine side chain to preserve the positive electrostatic environment, to test if the loss of activity is solely due to the loss of a positive charge. Thus, adding back a positive charge led to an increase in K_m of 9-fold compared to that of R404A (Table 2). The K_m value is consistent with a previous proposal that the repulsion between the Arg404 side chain and the positively charged arginine group of the substrate causes the high K_m of the wild-type enzyme. However, the activity was not recovered from R404K with simply addition of a positive charge on the side chain.

Obviously, Arg404 must play a critical role in the hydrolysis of the substrate. Sequence alignments show that Arg404 is conserved in AMPPs from *E. coli*, *Streptomyces lividans*, and *Mycobacterium tuberculosis* and in prolidases from humans or *E. coli* (Figure 2). In addition, the pH profile of wild-type and mutant R404A exhibited a similar pH dependence of log k_{cat}, although the catalytic activity of the mutant is much lower at all pH values. The pH profiles verify that the alkaline pK_a does not belong to Arg404. Therefore, Arg404 may be involved in other specific functions rather than playing a role as a general base.

The question of whether the Arg404 residue facilitates the ability of Asp260 to bind manganese is interesting. The X-ray structure of AMPP suggests that Asp260, Asp271, and Glu406 coordinate to Mn_B and that Asp260 is bound in a bidentate fashion. The ζ1 nitrogen from the guanidinium side chain of Arg404 is 2.9 Å from the nearest oxygen of the Asp260 carboxylate side chain. Thus, Arg404 may play a role in the stabilization of Asp260 coordinated to Mn_B via a

hydrogen bonding interaction. In contrast, R404A may not play a similar role. However, the results of ICP-MS experiments indicate that R404A, like the wild-type enzyme, contains two manganese ions per monomer of the protein. Therefore, this hypothesis seems unlikely since the R404A mutant, which has no capability to hydrogen bond to Asp260, still contains two manganese ions properly.

Another question concerns how the Arg404 residue influences protein structure. Since the R404L mutant aggregates during purification, it appears that the arginine side chain influences stabilization of the protein structure. Because the buried Arg404 residue can form intramolecular hydrogen bonds or salt bridges with neighboring polar groups that are also solvent inaccessible (e.g., Asp260), this residue may function to stabilize the native state of the enzyme by alleviating the energy associated with burying a charged side chain in the hydrophobic protein interior (*26*). However, the CD spectrum of R404A can be superimposed on that of the native enzyme, suggesting that the formation of the cavity does not substantially affect the secondary structure of the protein (Figure 5). Hence, the catalytic deficiencies of these mutants, R404A and R404K, cannot be attributed to pertubation of the overall enzyme structure.

A final question concerns the possible participation of the AMPP Arg404 residue in a proton relay system. Analysis of the crystal structure of AMPP with an inhibitor bound led to the proposal that the side chain carboxylate of Glu383 stabilizes the metal-bridging hydroxide in the active site via hydrogen bonding. It is suggested that, following cleavage of the peptide bond, several residues may shuttle a proton from bulk solvent to the dinuclear center, where protonation of the leaving peptide takes place (*8*, *10*). Although the spectroscopic properties of AMPP closely resemble these reported for arginase (*7*, *27*), Wilce and his colleagues (*8*) found that an equivalent Mn_A His101···Ser230···Asp274 hydrogen bond network found in arginase (*28*, *29*) does not exist in the active site of AMPP. However, the results of our kinetic measurement suggest that Arg404 and Tyr387 do participate with the Mn_B Asp260···Arg404···Tyr387 motif in a hydrogen-bonded network that could shuttle a proton from bulk solvent to the leaving peptide (Figure 7A). In fact, mutation of Arg404 to alanine or lysine, each of which is incapable of participation in proton transfer, leads to retention of only 0.2 and 0.4% of the catalytic activity compared to that of the wild-type enzyme. A reasonable explanation for the decreased k_{cat} of the R404K mutant might be that the lysine residue is not capable of forming a hydrogen bond required for its role in facilitating proton transfer in dual directions (Figure 7B). Obviously, the fact that the guanidinium group of Arg404 plays an important role in catalytic activity might be a consequence of its ability to govern the direction of proton transfer between Asp260 and Tyr387. The cavity created by replacing arginine with alanine enables the rescue of the catalytic activity of R404A seen by the addition of guanidine. Significantly, the activity of the R404A mutant can be enhanced more than 2- or 6-fold when 7.5 or 75 μM guanidine, respectively, is added. R404K shows no enhancement in catalytic activity with the addition of guanidine because guanidine is too large to fit into the cavity that is created by this mutation.

The enhancement of activity with guanidine added during the assembly of the active site within R404A suggests that guanidine itself is capable of acting as a hydrogen bond bridge between Asp260 and Tyr387 (Figure 7C). Additional support for this suggestion is found in the results of kinetic studies with the mutants derived by changing Tyr387. For example, the Y387F mutant has a 16-fold smaller k_{cat} value compared to that of the wild-type enzyme. Invoking the suppression of a direct proton transfer pathway between Arg404 and Y387F can account for this effect. These results suggest that a proton can be shuttled from solvent to the leaving peptide with the assistance of Arg404 and Tyr387 as depicted in Figure 8.

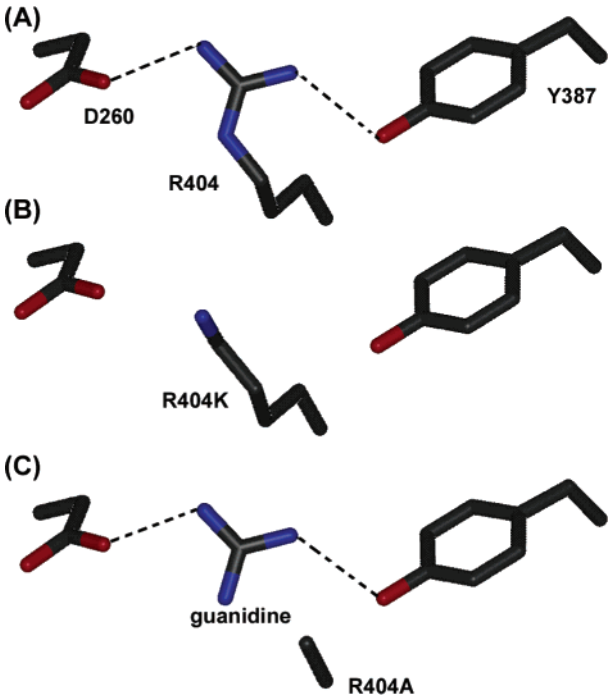

FIGURE 7: Comparison of the orientation of the guanidinium group of Arg404 interacting with the γ-carboxylate of Asp260 and the η-hydroxyl of Tyr387 in (A) the wild-type AMPP crystal structure, (B) the modeled structure displaying the relative position of R404K, and (C) the modeled structure showing the R404A substitution with guanidine forming hydrogen bond interactions with two neighboring residues. The hydrogen bonding interactions are shown as dashed lines.

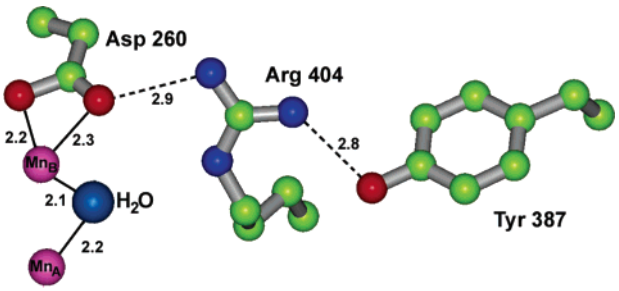

FIGURE 8: Hydrogen bond network in the active site of AMPP formed by Asp260, Arg404, and Tyr387. Distances (angstroms) are shown as dashed lines. The figure was created with InsightII from atomic coordinates of PDB entry 1A16.

ACKNOWLEDGMENT

We thank W. H. Chang at the Instrument Center of Hsinchu in National Tsing Hua University for performing the ICP-MS experiments.

REFERENCES

1. Yoshimoto, T., Orawski, A. T., and Simmons, W. H. (1994) Substrate specificity of aminopeptidase P from *Escherichia coli*: Comparison with membrane-bound forms from rat and bovine lung, *Arch. Biochem. Biophys. 311*, 28−34.
2. Yoshimoto, T., Murayama, N., Honda, T., Tone, H., and Tsuru, D. (1988) Cloning and expression of aminopeptidase P gene from *Escherichia coli* HB101 and characterization of expressed enzyme, *J. Biochem. 104*, 93−97.
3. Yaron, A., and Mlynar, D. (1968) Aminopeptidase-P, *Biochem. Biophys. Res. Commun. 32*, 658−663.
4. Bazan, J. F., Weaver, L. H., Roderick, S. L., Huber, R., and Matthews, B. W. (1994) Sequence and structure comparison suggest that methionine aminopeptidase, prolidase, aminopeptidase P, and creatinase share a common fold, *Proc. Natl. Acad. Sci. U.S.A. 91*, 2473−2477.
5. Lowther, W. T., and Matthews, B. W. (2002) Metalloaminopeptidases: Common functional themes in disparate structural surroundings, *Chem. Rev. 102*, 4581−4607.
6. Cunningham, D. F., and O'Connor, B. (1997) Proline specific peptidases, *Biochim. Biophys. Acta 1343*, 160−186.
7. Zhang, L., Crossley, M. J., Dixon, N. E., Ellis, P. J., Fisher, M. L., King, G. F., Lilley, P. E., MacLachlan, D., Pace, R. J., and Freeman, H. C. (1998) Spectroscopic identification of a dinuclear metal center in manganese(II)-activated aminopeptidase P from *Escherichia coli*: Implications for human prolidase, *J. Biol. Inorg. Chem. 3*, 470−483.
8. Wilce, M. C. J., Bond, C. S., Dixon, N. E., Freeman, H. C., Guss, J. M., Lilley, P. E., and Wilce, J. A. (1998) Structure and mechanism of a proline-specific aminopeptidase from *Escherichia coli*, *Proc. Natl. Acad. Sci. U.S.A. 95*, 3472−3477.
9. Graham, S. C., Lee, M., Freeman, H. C., and Guss, J. M. (2003) An orthorhombic form of *Escherichia coli* aminopeptidase P at 2.4 Å resolution, *Acta Crystallogr. D59*, 897−902.
10. Graham, S. C., Maher, M. J., Simmons, W. H., Freeman, H. C., and Guss, J. M. (2004) Structure of *Escherichia coli* aminopeptidase P in complex with the inhibitor apstatin, *Acta Crystallogr. D60*, 1770−1779.
11. Roderick, S. L., and Matthews, B. W. (1993) Structure of the cobalt-dependent methionine aminopeptidase from *Escherichia coli*: A new type of proteolytic enzyme, *Biochemistry 32*, 3907−3912.
12. Liu, S., Widom, J., Kemp, C. W., Crews, C. M., and Clardy, J. (1998) Structure of human methionine aminopeptidase-2 complexed with fumagillin, *Science 282*, 1324−1327.
13. Lowther, W. T., Zhang, Y., Sampson, P. B., Honek, J. F., and Matthews, B. W. (1999) Insights into the mechanism of *Escherichia coli* methionine aminopeptidase from the structural analysis of reaction products and phosphorus-based transition-state analogues, *Biochemistry 38*, 14810−14819.
14. Oefner, C., Douangamath, A., D'Arcy, A., Hafeli, S., Mareque, D., MacSweeney, A., Padilla, J., Pierau, S., Schulz, H., Thormann, M., Wadman, S., and Dale, G. E. (2003) The 1.15 Å crystal structure of the *Staphylococcus aureus* methionyl-aminopeptidase and complexes with triazole based inhibitors, *J. Mol. Biol. 332*, 13−21.
15. Hoeffken, H. W., Knof, S. H., Bartlett, P. A., Huber, R., Moellering, H., and Schumacher, G. (1988) Crystal structure determination, refinement and molecular model of creatine amidinohydrolase from *Pseudomonas putida*, *J. Mol. Biol. 204*, 417−433.
16. Coll, M., Knof, S. H., Ohga, Y., Messerschmidt, A., Huber, R., Moellering, H., Ruessmann, L., and Schumacher, G. (1990) Enzymic mechanism of creatine amidinohydrolase as deduced from crystal structures, *J. Mol. Biol. 214*, 597−610.
17. Yoshimoto, T., Tanaka, N., Kanada, N., Inoue, T., Nakajima, Y., Haratake, M., Nakamura, K. T., Xu, Y., and Ito, K. (2004) Crystal structures of creatininase reveal the substrate binding site and provide an insight into the catalytic mechanism, *J. Mol. Biol. 337*, 399−416.
18. Yaron, A., and Naider, F. (1993) Proline-dependent structural and biological properties of peptides and proteins, *Crit. Rev. Biochem. Mol. Biol. 28*, 31−81.
19. Willingham, K., Maher, M. J., Grunden, A. M., Ghosh, M., Adams, M. W. W., Freeman, H. C., and Guss, J. M. (2001) Crystallization and characterization of the prolidase from *Pyrococcus furiosus*, *Acta Crystallogr. D57*, 428−430.
20. Maher, M. J., Ghosh, M., Grunden, A. M., Menon, A. L., Adams, M. W. W., Freeman, H. C., and Guss, J. M. (2004) Structure of the prolidase from *Pyrococcus furiosus*, *Biochemistry 43*, 2771−2783.
21. Kitazono, A., Kabashima, T., Huang, H.-S., Ito, K., and Yoshimoto, T. (1996) Prolyl aminopeptidase gene from *Flavobacterium meningosepticum*: Cloning, purification of the expressed enzyme, and analysis of its sequence, *Arch. Biochem. Biophys. 336*, 35−41.
22. Prechel, M. M., Orwaski, A. T., Maggiora, L. L., and Simmons, W. H. (1995) Effect of a new aminopeptidase P inhibitor, apstatin, on bradykinin degradation in the rat lung, *J. Pharmacol. Exp. Ther. 275*, 1136−1142.
23. Ersahin, C., and Simmons, W. H. (1997) Inhibition of both aminopeptidase P and angiotensin-converting enzyme prevents bradykinin degradation in the rat coronary circulation, *J. Cardiovasc. Pharmacol. 30*, 96−101.
24. Jao, S.-C., Huang, L.-F., Tao, Y. S., and Li, W.-S. (2004) Hydrolysis of organophosphate triesters by *Escherichia coli* aminopeptidase P, *J. Mol. Catal. B: Enzym. 27*, 7−12.
25. Gasteiger, E., Hoogland, C., Gattiker, A., Duvaud, S., Wilkins, M. R., Appel, R. D., and Bairoch, A. (2005) Protein Identification and Analysis Tools on the ExPASy Server, in *The Proteomics Protocols Handbook* (Walker, J. M., Ed.) pp 571−607, Humana Press, Totowa, NJ.
26. Anderson, D. E., Backtel, W. J., and Dahlquist, F. W. (1990) pH-induced denaturation of proteins: A single salt bridge contributions 3−5 kcal/mol to the free energy of folding of T4 lysozyme, *Biochemistry 29*, 2403−2408.
27. Khangulov, S. V., Pessiki, P. J., Barynin, V. V., Ash, D. E., and Dismukes, G. C. (1995) Determination of the metal ion separation and energies of the three lowest electronic states of dimanganese-(II,II) complexes and enzymes: Catalase and liver arginase, *Biochemistry 34*, 2015−2025.
28. Scolnick, L. R., Kanyo, Z. F., Cavalli, R. C., Ash, D. E., and Christianson, D. W. (1997) Altering the binuclear manganese cluster of arginase diminishes thermostability and catalytic function, *Biochemistry 36*, 10558−10565.
29. Kanyo, Z. F., Scolnick, L. R., Ash, D. E., and Christianson, D. W. (1996) Structure of a unique binuclear manganese cluster in arginase, *Nature 383*, 554−557.

BI051786M